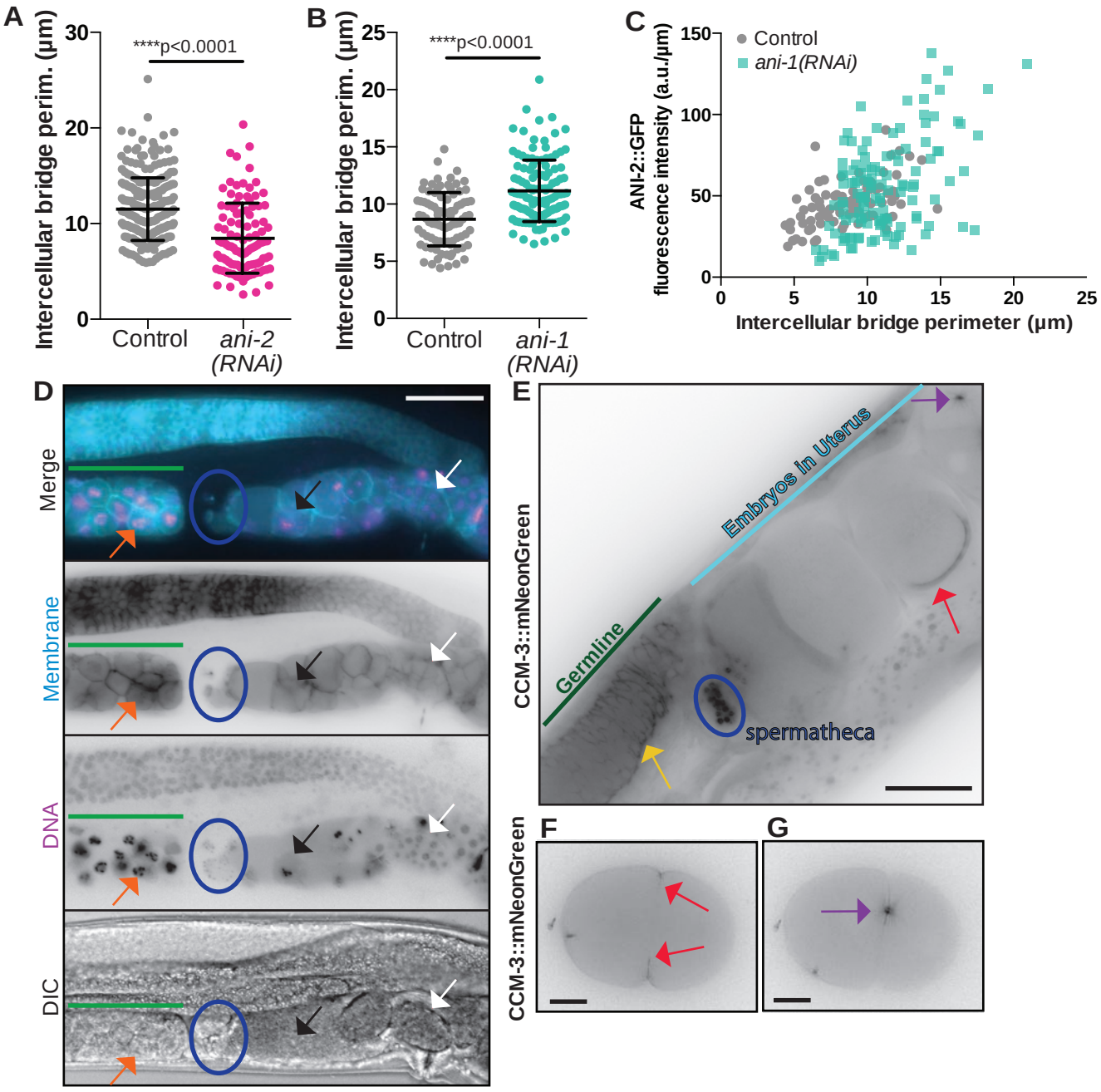
A
Intercellular bridge perim. (µm)
****p<0.0001
Control
ani-2 (RNAi)
B
Intercellular bridge perim. (µm)
****p<0.0001
Control
ani-1 (RNAi)
C
Control
ani-1(RNAi)
ANI-2::GFP fluorescence intensity (a.u./µm)
Intercellular bridge perimeter (µm)
D
Merge
Membrane
DNA
DIC
E
CCM-3::mNeonGreen
Embryos in Uterus
Germline
spermatheca
F
G
CCM-3::mNeonGreen

Figure S1: Regulation of germline structure and function by ANI-1, ANI-2, GCK-1, and CCM-3. Related to Figure 2.

(A) Intercellular bridge perimeter in control (n=258 bridges) and ANI-2 depleted (n=105) worms. Intercellular bridge size was significantly decreased relative to controls (****p<0.0001).

(B) Intercellular bridge perimeter in control (n=89 bridges) and ANI-1 depleted (n=125) worms. Intercellular bridge size was significantly increased relative to controls (****p<0.0001).

(C) Average fluorescence intensity (a.u./µm) of ANI-2::GFP on intercellular bridges versus intercellular bridge perimeter (µm) in control (n=89) and ANI-1 depleted (n=125) germlines. Intercellular bridge perimeter was significantly increased following ANI-1 depletion relative to controls (****p<0.0001). Average fluorescence intensity of ANI-2::GFP was significantly increased following ANI-1 depletion relative to controls (**p=0.0032). Spearman coefficients: control=0.4826 ***p<0.001; *ani-1(RNAi)*=0.4186 ****p<0.0001.

(D) Representative images (maximum intensity projections) of intact germlines in *gck-1(RNAi)* MDX27 worms where GFP:: PLCδ-PH labels the plasma membrane and mCherry::HIS-58 marks DNA. In 6 of 9 *gck-1(RNAi)* worms, compared to 0 of 8 control worms, we observed what appear to be unfertilized cells (black arrow) in the uterus (to the right of the spermatheca; blue oval). These cells have DNA morphology similar to cells (orange arrow) in the proximal gonad arm (green line). The cells appear to be unfertilized as they lack the eggshell, which is formed upon fertilization, visible around embryos (white arrow) via differential interference contrast (DIC) microscopy.
Scale bar = 20 µm.

(E) Representative image (maximum intensity projections) of CCM-3::mNeonGreen localization in an intact (in worm) C. elegans germline (green line), and in embryos in the uterus (light blue line). CCM-3::mNeonGreen localizes to intercellular bridges (yellow arrow) of the germline, sperm in the spermatheca (blue oval), and the cytokinetic ring (red arrow) and midbodies (purple arrow) in embryos. Scale bar = 20 µm.

(F) Localization of CCM-3::mNeonGreen to the cytokinetic ring (red arrow) in an isolated embryo (maximum intensity projection). Scale bar = 10 µm.

(G) Localization of CCM-3::mNeonGreen to the midbody (purple arrow) in an isolated embryo (maximum intensity projection). Scale bar = 10 µm.

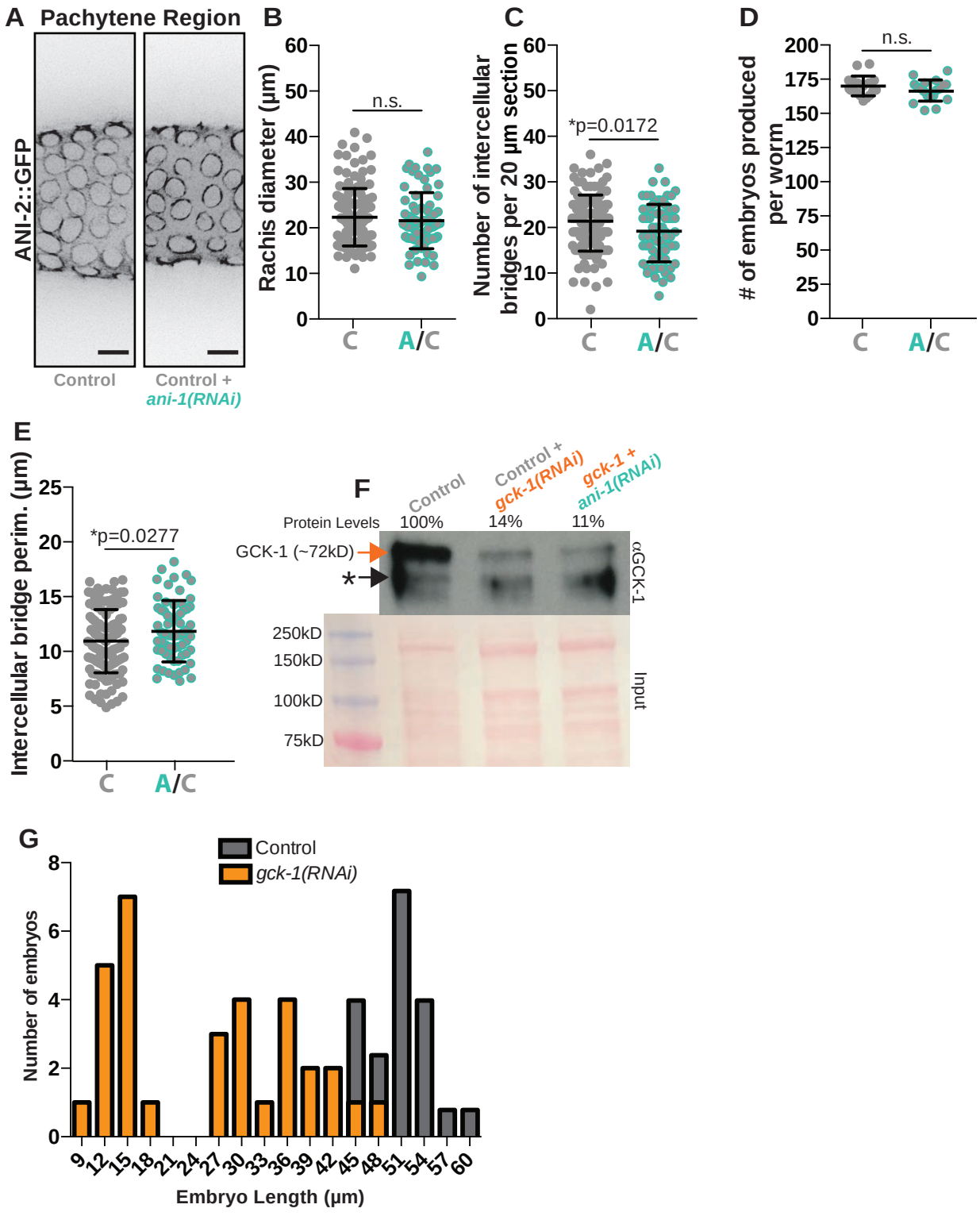
A
Pachytene Region
ANI-2::GFP
Control
Control +
ani-1(RNAi)
B
Rachis diameter (µm)
n.s.
C
A/C
C
Number of intercellular bridges per 20 µm section
*p=0.0172
D
# of embryos produced per worm
n.s.
E
Intercellular bridge perim. (µm)
*p=0.0277
F
Control
Control + gck-1(RNAi)
gck-1 + ani-1(RNAi)
Protein Levels
100%
14%
11%
GCK-1 (~72kD)
αGCK-1
250kD
150kD
100kD
75kD
Input
G
Control
gck-1(RNAi)
Number of embryos
Embryo Length (µm)

Figure S2: Controls related to co-depletion of ANI-1 with both control(RNAi) and gck-1(RNAi). Related to Figure 3.

A) Representative images (maximum intensity projections) of intercellular bridges labeled with ANI-2::GFP in control and “single” depletion (*ani-1(RNAi)*+control) worms. Scale bars = 5 µm.

B) Average rachis diameter for 20 µm sections of pachytene in control (n=127 sections) and “single” depletion *ani-1(RNAi)*+control (n=72) germlines. Rachis diameter is not significantly changed between the two conditions (p=0.4182).

C) Number of intercellular bridges per 20 µm section of pachytene length in control (n=126 sections), “single” depletion *ani-1(RNAi)*+control (n=71) worms. The number of intercellular bridges per section is significantly reduced in *ani-1(RNAi)*+control germlines compared to controls (*: p=0.0172).

D) Number of embryos produced per worm in 48 hours by control (n=20 worms) and “single” depletion *ani-1(RNAi)*+control (n=19) worms. Brood size was not significantly different between the two conditions (p=0.1745).

E) Average intercellular bridge perimeter for 20 µm sections of the pachytene region of the germline in control (n=127 sections) and “single” depletion *ani-1(RNAi)*+control (n=70) worms. Intercellular bridge size was significantly increased in *ani-1(RNAi)*+control germlines compared to controls (*p=0.0277).

(F) Western blot of whole worm lysates from control, *gck-1(RNAi)*+control, and *gck-1+ani-1(RNAi)* conditions probed with a GCK-1 specific antibody. A Ponceau S stained blot is included as a loading control. GCK-1 protein levels (indicated by orange arrow) were reduced to 14% and 11% of controls following *gck-1(RNAi)*+control and *gck-1+ani-1(RNAi)* respectively. * indicates non-specific/non-depleted bands.

(G) Histogram of embryo length in control (n=24 embryos) and *gck-1(RNAi)* (n=32) conditions. Data are compiled into 3 µm bins from 9 µm to 60 µm. Embryo length from the *gck-1(RNAi)* has a bimodal distribution.

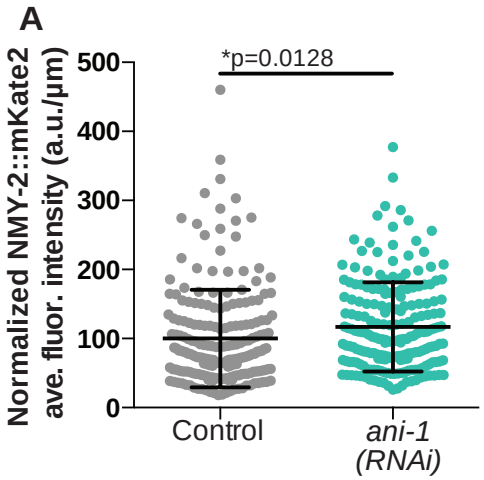
A
Normalized NMY-2::mKate2 ave. fluor. intensity (a.u./µm)
*p=0.0128
500
400
300
200
100
0
Control
ani-1 (RNAi)

Figure S3: NMY-2::mKate2 localization on intercellular bridges following ani-1(RNAi). Related to Figure 4.

(A) Normalized NMY-2::mKate2 average fluorescence intensity (a.u./µm) in control (n=200 bridges) and *ani-1(RNAi)* (n=206) germlines. NMY-2::mKate2 average fluorescene intensity is slightly increased following ANI-1 depletion (*p=0.0128).

accession number	gene name	max coverage	Embryo/ Larva/Adult	function/protein type
F27C1.7	*atp-3*	22.2%	EL	mitochondrial ATP synthesis
D2024.6	*cap-1*	11.0%	L	F-actin capping protein
Y25C1A.5	*copb-1*	9.5%	E	COPI vesicle coat
T26A5.9	*dlc-1*	57.3%	EL	dynein light chain
F17C11.9	*eef-1G*	28.4%	EL	translation elongation factor
ZK328.2	*eftu-2*	12.6%	EL	GTP binding, translation elongation
T19A5.2	***gck-1***	**32.8%**	**ELA**	**serine/threonine kinase**
C26D10.2	*hel-1*	18.8%	EL	mRNA export
T25G12.4	*rab-6.2*	13.2%	A	GTP binding, membrane traffic
D1037.4	*rab-8*	10.4%	L	GTP binding, membrane traffic
K01G5.4	*ran-1*	11.2%	L	nuclear transport, microtubule dynamics
T05G5.7	*rmd-1*	17.1%	LA	apoptosis, microtubule-binding
F10B5.1	*rpl-10*	10.7%	L	ribosomal subunit
T22F3.4	*rpl-11.1*	12.8%	L	ribosomal subunit
C04F12.4	*rpl-14*	14.8%	L	ribosomal subunit
C14B9.7	*rpl-21*	17.4%	L	ribosomal subunit
C27A2.2	*rpl-22*	17.7%	LA	ribosomal subunit
Y106G6H.3	*rpl-30*	29.2%	L	ribosomal subunit
F37C12.9	*rps-14*	19.1%	A	ribosomal subunit
F39B2.6	*rps-26*	20.5%	L	ribosomal subunit
ZC434.2	*rps-7*	17.0%	L	ribosomal subunit
C52E4.3	*snr-4*	17.8%	A	RNA splicing, apoptosis
Y49E10.15	*snr-6*	27.8%	L	P granule, snRNP biogenesis
Y116A8C.35	*uaf-2*	15.4%	EL	RNA binding
C35D10.13		15.5%	L	apoptosis
F43D9.3		10.9%	EL	apoptosis, human SCFD1 homologue
K07C5.4		22.0%	EL	box C/D snoRNP complex

Table S1: Curated list of ANI-1 immunoprecipitation hits. Related to Figure 2.
Proteins with at least 10% sequence coverage that were a) detected by tandem mass spectrometry in one to three ANI-1 immunoprecipitations, b) present in the collection of proteins required for germline function, and c) not present in a negative control (GST) IP.

Supplemental Experimental Procedures

C. elegans strains and culture

Worm strains were maintained at 20°C using standard procedures [S1]. The strains utilized in this work are listed in the table below.

C. elegans *strains*

Strain	Genotype
N2	Wild-type Bristol strain
MDX29	*ani-1(mon7[mNeonGreen^3xFlag::ani-1]) III*
UM208 [2]	*unc-119(ed3) III; ltIs81 [Ppie-1::gfp-TEV-Stag::ani-2; unc-119 (+)]; ltIs44 [Ppie-1::mCherry::PH(PLC1delta1); unc-119(+)] IV*
MDX38	*ccm-3(mon9[ccm-3::mNeonGreen^3xFlag]) II*
LP229	*nmy-2(cp52[nmy-2::mkate2 + LoxP unc-119(+) LoxP]) I; unc-119 (ed3) III*
MDX40	MDX29 x LP229
MDX27	*cpIs53[Pmex-5::GFP-C1::PLCδ-PH::tbb-2 3'UTR + unc-119 (+)] II; unc-119(ed3) III, ltIs37 [pAA64; pie-1/mCherry::his-58; unc-119 (+)] IV*

RNA-mediated interference

Both single and double depletions were conducted using nematode growth media (NMG) plates containing IPTG and ampicillin seeded with the HT115 bacteria strain containing the L4440 vector for IPTG mediated induction of dsRNA expression as described [S2]. Individual bacterial clones from the Arhinger library [S3] were kindly provided by Jean-Claude Labbé (IRIC, Université de Montréal) and Bob Goldstein (University of North Carolina at Chapel Hill). The targets of all clones used in this study were confirmed by sequencing. Bacterial cultures were grown overnight to saturation. Cultures were then diluted 1:100 and grown at 37°C for 4hrs to return bacteria to log phase growth. Cultures were then diluted to an OD600 of 0.6 and used to seed NMG plates. For double depletions, equal amounts of two dsRNA-expressing bacterial strains were mixed before seeding. To control for the second RNAi target in the double depletions, "single" depletions were performed with a dilution control of dsRNA targeting mCherry. All double depletion experiments were done in a *C. elegans* strain (UM208) exogenously expressing mCherry::PH(PLC1-δ1), a non-essential foreign gene [S3]. All RNAi experiments were conducted by placing 10-15 L4 worms on RNAi plates and allowing the worms to feed for either 24 hrs (GCK-1, CCM-3, LET-502) or 48 hrs (ANI-1, ANI-2, ANI-1/control, GCK-1/control, CCM-3/control, GCK-1/ANI-1, CCM-3/ANI-1). Longer depletion times (48hrs) were used for double depletions as having two targets reduced depletion efficiency and for more stable proteins, such as ANI-1 and ANI-2, since shorter-term depletions (24hrs) do not result in a measurable phenotype.

Extruded gonad imaging and analysis

Several adult worms (4-5) were picked into 10µl of M9 buffer + 100 ng/mL DAPI (4',6'-diamidino-2-phenylindole hydrochloride) on a 0.1% poly-L-lysine coated cover slip. Gonads were extruded by cutting just behind the pharynx. The sample was mounted by applying a small mound of Vaseline to the corners of the coverslip and then placing the coverslip gently onto a slide. The mounds of Vaseline prevent excess compression oL4f the extruded gonads. Images were acquired with a CoolSnap Hq camera (Photometrics) mounted on a DeltaVision Image Restoration System (GE). A 60x/1.42 NA Plan Apochromat objective was used to acquire Z-stacks with 500 µm spacing through the entire gonad thickness. Images were then deconvolved (10 cycles of enhanced ratio with medium noise filtering) using the softWoRx 5.5 software (Applied Precision).

Images were processed with the ImageJ based software FIJI [S4]. Max projections of z-slices through the top half of the gonad were generated to visualize intercellular bridges *en face.* The gonad was then segregated into 20 µm sections starting at the distal tip and continuing through to the proximal arm. The meiotic stage of cells within each section was determined based on chromatin morphology as described [S5]. Intercellular bridge perimeter and average fluorescence intensity measurements were made in Fiji (ImageJ) by hand tracing a two-pixel wide line around the bridge through the middle of a prominent bridge marker. A local cytoplasmic background intensity measurement taken from the center of each bridge was subtracted from the average fluorescence intensity of the pixels contained within the two-pixel wide trace.

The widest portion of the rachis was measured in each section to determine rachis diameter. The number of intercellular bridges in each 20 μm section was hand counted. Any partially visible rings at the edges of the rachis were excluded from the bridge number and perimeter measurements.

In worm germline, uterus and embryo imaging and analysis

Intact worms were mounted in 10 μl of M9 + sodium azide (final concentration 20mM) on 0.1% poly-L-lysine coated cover slips with Vaseline spacers and imaged as above. Embryo length was measured along the longest embryo axis from a single z-plane of the DIC image stack.

Brood size analysis

10-15 N2 worms at the fourth larval stage (L4) were placed on NGM plates seeded with bacteria expressing dsRNAs (as described above) for 24 hrs, during which time they became adults and began producing progeny. Worms were then singled onto individual plates and allowed to lay for 24hrs. At the end of this time the adults were moved to a fresh plate (1 worm per plate) and allowed to lay for another 24hrs. Finally, adult worms were removed from the plates and the number of progeny (embryos and larvae) on each plate (2 plates per worm) was counted. The totals from each plate were combined to determine the total number of offspring produced during the 48 hr period.

Statistical analysis

We applied the Student's *t* test using GraphPad PRISM to determine the statistical significance between sample conditions. Assumptions of normality and equal variance were met for all data analyzed. We considered a p value less than 0.05 from a two-tailed *t* test significant. All results are expressed as average ± Standard Deviation. Sample size (n) and p-values are given on each figure panel and/or in the figure legends.

Spearman and Pearson correlation coefficients, calculated using GraphPad PRISM, were used to assess the relationship between two variables. For Spearman coefficeints 95% confidence intervals and p-values are given in the figure panels and/or in the figure legends. For Pearson coefficients 95% confidence intervals, R-squared values, and p-values are given in the figure panels and/or in the figure legends.

Immunoprecipitation and mass spectrometry

Immunoprecipitations were performed as previously described [S6], with the addition of Cytochalasin B to the lysate to a final concentration of 110 μg/ml. Mass spectrometry was conducted essentially as described in [6], except tandem mass spectra were searched against the most recent version of the predicted *C. elegans* proteins (Wormpep 150).

Western blotting

Whole worm lysates were prepared as previously described [S7]. Immuno-blots were probed with polyclonal antibodies against GCK-1 (residues 452-636). Ponceau S staining of the blot was used to control for initial protein loading.

CRISPR/Cas9 genome editing

The strain LP229 (Goldstein lap unpublished) was generated using the CRISPR genome editing techniques as described [S8].The strain MDX38 was generated using an updated CRISPR genome editing technique as described [S9]. MDX29 was generated using an earlier version of the CRISPR methods described in (Dan Dickinson personal communication) specifically using shorter homology arms. MDX29 guide plasmids were generated as described in [S8,S9]. A repair DNA containing mNG, 3xFLAP, SEC cassette as well as 5' and 3' homology arms was generated by PCR. The primers used contained the entire homology sequences and no PAM site mutations were necessary. Injection mixes were prepared as described in [S9] but purified repair PCR was injected instead of a repair plasmid. The targeting sequence and primers for each strain are respectively listed in the tables below.

CRISPR/cas9 Targeting Sequences

Gene	Targeting Sequence
ani-1	ctacactgtaaatacaatggGGG
ccm-3	CATATGGGTGAGCTTATCCTCGG

Primer sequences

Primer	Sequence
ani-1 Cas9 Primer	ctacactgtaaatacaatggGTTTTAGAGCTAGAAATAGCAAGT
ani-1 5' Homology Primer	ggaaacattgttttcttgcagaactacactgtaaatacaATGGTCTCCAAGGGAGAG
ani-1 3' Homology Primer	tcgtatgcgttccattagagaatcgaattgatcccccatTCTCTTGTCATCGTCATCCTT
ccm-3 Cas9 Primer	CATATGGGTGAGCTTATCCTGTTTTAGAGCTAGAAATAGCAAGT
ccm-3 5' Homology Forward	ACGTTGTAAAACGACGGCCAGTCGCCGGCAACCATCAAGCTCATCGCATC
ccm-3 5' Homology Reverse	CATCGATGCTCCTGAGGCTCCCGATGCTCCTCCTCGTCGAAGTTTTTCG
ccm-3 3' Homology Forward	CGTGATTACAAGGATGACGATGACAAGAGATAAGCTCACCCATATGGCGGC
ccm-3 3' Homology Reverse	GGAAACAGCTATGACCATGTTATCGATTTCGCACAGCCCTGTTACCAACC

Supplemental References

S1. Brenner S. (1974). The genetics of Caenorhabditis elegans. Genetics *77*, 71–94.

S2. Amini R., Goupil E., Labella S., Zetka M., Maddox A.S., Labbé J.C., Chartier N.T. (2014) C. elegans Anillin proteins regulate intercellular bridge stability and germline syncytial organization. J. Cell Biol. *206*, 129–43.

S3. Kamath R.S., Martinez-Campos M., Zipperlen P., Fraser A.G., Ahringer J. (2001). Effectiveness of specific RNA-mediated interference through ingested double-stranded RNA in Caenorhabditis elegans. Genome Biol. *2*, research0002.1-0002.10.

S4. Schindelin J., Arganda-Carreras I., Frise E., Kaynig V., Longair M., Pietzsch T., Preibisch S., Rueden C., Saalfeld S., Schmid B., et al. (2012). Fiji: an open-source platform for biological-image analysis. Nat. Methods *9*, 676–82.

S5. Hillers K.J., Jantsch V., Martinez-Perez E., Yanowitz J.L. (2015). Meiosis. Wormbook 1-54.

S6. Cheeseman I.M., Niessen S., Anderson S., Hyndman F., Yates J.R., Oegema K., Desai A. (2004). A conserved protein network controls assembly of the outer kinetochore and its ability to sustain tension. Genes Dev. *18*, 2255–68.

S7. Hannak E., Kirkham M., Hyman A.A., Oegema K. (2001). Aurora-A kinase is required for centrosome maturation in Caenorhabditis elegans. J. Cell Biol. *155*, 1109-16.

S8. Dickinson D.J., Ward J.D., Reiner D.J., Goldstein B. (2013). Engineering the Caenorhabditis elegans genome using Cas9-triggered homologous recombination. Nat. Methods *10*, 1028–34.

S9. Dickinson D.J., Pani A.M., Heppert J.K., Higgins C.D., Goldstein B. (2015) Streamlined Genome Engineering with a Self-Excising Drug Selection Cassette. Genetics *200*, 1035–49.